Neurosecretory protein GL, a hypothalamic small secretory protein, participates in energy homeostasis in male mice

Daichi Matsuura, Kenshiro Shikano, Takaya Saito, Eiko Iwakoshi-Ukena, Megumi Furumitsu, Yuta Ochi, Manami Sato, George E. Bentley, Lance J. Kriegsfeld, and Kazuyoshi Ukena

Endocrinology
Endocrine Society

Submitted: January 14, 2017
Accepted: March 13, 2017
First Online: March 17, 2017

Neurosecretory protein GL, a hypothalamic small secretory protein, participates in energy homeostasis in male mice

Daichi Matsuura*, Kenshiro Shikano*, Takaya Saito*, Eiko Iwakoshi-Ukena, Megumi Furumitsu, Yuta Ochi, Manami Sato, George E. Bentley, Lance J. Kriegsfeld, and Kazuyoshi Ukena#

Section of Behavioral Sciences (D.M., K.S., T.S., E.I.-U., M.F., Y.O., M.S., K.U.), Graduate School of Integrated Arts and Sciences, Hiroshima University, Higashi-Hiroshima 739-8521, Japan

Department of Integrative Biology (E.I.-U., G.E.B.), The Helen Wills Neuroscience Institute, University of California at Berkeley, Berkeley, CA 94720-3140, USA, Department of Psychology (K.U., L.J.K.), The Helen Wills Neuroscience Institute, University of California at Berkeley, Berkeley, CA 94720-3140, USA

Received 14 January 2017. Accepted 13 March 2017.

*D.M., K.S. and T.S. contributed equally to this work.

We have recently identified a novel cDNA encoding a small secretory protein termed neurosecretory protein GL (NPGL) from the avian hypothalamus. In chicks, NPGL increases body weight gain without affecting food intake. A database search reveals that NPGL is conserved throughout vertebrates. However, the central distribution and functional role of NPGL remains to be elucidated in mammals. In this study, we identified the precursor cDNA encoding NPGL from the mouse hypothalamus. Quantitative RT-PCR and morphological analyses revealed that *NPGL* precursor mRNA is robustly expressed in the mediobasal hypothalamus with NPGL neurons specifically localized to the lateroposterior part of the arcuate nucleus in the hypothalamus. NPGL-immunoreactive fibers were observed in close anatomical contact with pro-opiomelanocortin neurons in the rostral region of the arcuate nucleus. *NPGL* mRNA expression was elevated by 24 h fasting and reduced by feeding of a high fat diet for 5 weeks. Furthermore, intracerebroventricular injection of mature NPGL increased food intake, pointing to an important role in feeding. Together, these findings provide the first report on the distribution of NPGL in the mammalian brain and point to an important role for this neuropeptide in energy homeostasis.

Abbreviations

NPGL, neurosecretory protein GL; POMC, pro-opiomelanocortin; NPY, neuropeptide Y; AgRP, agouti-related protein; DIO, diet-induced obesity; MBH, the mediobasal hypothalamus; ArcLP, the lateroposterior part of the arcuate nucleus; VMH, the ventromedial hypothalamus; DMH, the dorsomedial hypothalamus; HFD, high fat diet; Socs3, suppressor of cytokine signaling 3

This report represents the first characterization of precursor protein, localization, distribution, and biological action of neurosecretory protein GL (NPGL) in the mouse hypothalamus.

Introduction

The discovery of leptin, an anorexigenic peptide hormone secreted from adipose tissues (1), helped to clarify the means by which body composition is communicated to central structures that regulate feeding and metabolism. Leptin exerts its effect via two major neuronal populations, i.e., orexigenic neuropeptide Y (NPY)/agouti-related protein (AgRP) neurons and anorexigenic pro-opiomelanocortin (POMC) neurons in the arcuate nucleus (Arc) of the hypothalamus (2). In addition to leptin, ghrelin, an orexigenic peptide hormone secreted mainly from the gastric tissue, acts on NPY/AgRP neurons (3) to increase feeding. Feeding is further controlled by hypothalamic orexin, also called hypocretin, cells that are directly targeted by leptin and ghrelin (4). In turn, orexin cells innervate a number of neuronal phenotypes, including histaminergic, serotonergic and dopaminergic neurons (4). Despite considerable progress in understanding the regulation of hunger and satiety over the last several decades, the neural control of feeding is not completely understood. To further understand of the mechanism regulating feeding behavior, we sought to identify previously unknown hypothalamic neuropeptides.

To find novel neuropeptide precursors in the vertebrate brain, we performed a cDNA subtractive screen of the chicken hypothalamic infundibulum which contains one of the feeding centers in this species. After sequencing 596 clones, we identified a novel cDNA encoding a previously unknown small protein and termed this neurochemical neurosecretory protein GL (NPGL) because the precursor protein contained a secretory signal sequence at the N-terminus and the predicted C-terminal amino acids of the small protein were Gly-Leu-NH_2 (5). In chicks, subcutaneous chronic infusion of NPGL induces a significant increase in body weight gain without affecting food intake, suggesting a central role for this protein in regulating growth in this species (5). A database search revealed that the gene for NPGL is conserved in vertebrates, including human, rat and mouse. Given the role of NPGL in chick body weight regulation, we speculated that the mammalian homolog of NPGL might play an important role in feeding and/or energy metabolism. As a result, the present investigation sought to characterize whether NPGL is in a position to interact with well-established feeding circuitry and impact food intake. To accomplish this goal, we first cloned the cDNA encoding NPGL from the mouse hypothalamus and investigated the distribution of NPGL neurons throughout the brain. To explore the role of NPGL in monitoring energetic state, the expression of *NPGL* precursor mRNA was examined during fasting and in animals provided

with a high fat diet (HFD). Finally, the role of NPGL on feeding was explored by investigating the effect of intracerebroventricular (i.c.v.) injections of NPGL on food intake.

Materials and Methods

Animals

C57BL/6J mice were purchased from Charles River Laboratories (Kanagawa, Japan) and housed in standard conditions (23 ± 2°C under a 12hr light/12hr dark cycle) with *ad libitum* access to water and normal chow (CE-2; CLEA Japan, Tokyo, Japan). Mice fed HFD (D12492; Research Diets, New Brunswick, NJ) for either 5 or 13 weeks beginning at 4 weeks of age were also purchased from Charles River Laboratories. All animal experiments were performed according to the Guide for the Care and Use of Laboratory Animals prepared by Hiroshima University (Higashi-Hiroshima, Japan).

Molecular cloning of cDNA encoding NPGL

Male mice (8 weeks old) were used. The method used to clone *NPGL* have been described previously (6–9) and are briefly described herein. Preliminary results revealed that the *NPGL* precursor mRNA was highly expressed in the mediobasal hypothalamus (MBH). Therefore, cDNA synthesized from total RNA in the MBH was used as a source for cloning. Primers were designed based on the genomic sequence data (chromosome 1; accession no. AL645534). For cloning the 5' region, cDNA was amplified with the first primer: 5'-TCTAAGGAGCTGAGAATATGCA-3' (nucleotide no. 72,675-72,654) and the oligo dT anchor primer supplied in the 5'/3' rapid amplification of cDNA ends (RACE) kit (Roche Diagnostics, Basal, Switzerland). First-round PCR products were re-amplified with the second primer: 5'-TTAGAAACACGAGGCTTCC-3' (nucleotide no. 68,693-68,675) and the anchor primer. For cloning the 3' region, cDNA was amplified with the first primer: 5'-CACAGTCAGACAGACCTGC-3' (nucleotide no. 68,593-68,611) and the anchor primer. First-round PCR products were re-amplified with the second primer: 5'-CTGCTGACTCTTAACCAAGC-3' (nucleotide no. 68,608-68,627) and the anchor primer. These second-round PCR products were subcloned into a TA-cloning vector (pGEM-T Easy; Promega Corp., Madison, WI) in accordance with the manufacturer's instructions. The DNA inserts of the positive clones were amplified by PCR with universal M13 primers. The nucleotide sequence was determined using an ABI PRISM Dye terminator cycle sequencing ready reaction kit (Applied Biosystems, Foster City, CA) and a model 310 automated DNA sequencer (Applied Biosystems), and then analyzed with DNASIS-Pro software (Hitachi Software Engineering, Kanagawa, Japan). Universal M13 primers or gene-specific primers were used to sequence both strands.

Real-time RT-PCR

Male mice (8 weeks old) were sacrificed to examine the distribution of *NPGL* mRNA throughout the brain (telencephalon, diencephalon, mesencephalon, cerebellum, and MBH). In addition, the MBH from mice (9 and 17 weeks old) fed HFD for 5 and 13 weeks were also used. The tissues were frozen in liquid nitrogen and stored at –80°C for RNA processing. Total RNA was isolated with TRIzol regent (Life Technologies, Carlsbad, CA). RNA concentration was measured by nanodrop spectroscopy (Thermo Fisher Scientific, Waltham, MA), and cDNA was reverse-transcribed using ReverTra ACE qPCR RT Master Mix with gDNA Remover (TOYOBO, Osaka, Japan). PCR amplifications were performed with the THUNDERBIRD SYBR qPCR Mix (TOYOBO) using following conditions; 95°C for 20 s, followed by 40 cycles of 95°C for 3 s, and 60°C for 30 s. β-actin (ACTB) was used as endogenous controls. The following primers were used: *NPGL* sense primer; 5'-GGAACCATGGCTTAGGAAGG-3' (nucleotide no. 326-345 from the ATG initiation codon) and *NPGL* antisense primer; 5'-TCTAAGGAGCTGAGAATATGCA-3' (nucleotide no. 435-414), *suppressor of cytokine signaling 3* (*Socs3*) sense primer; 5'-ACCAGCGCCACTTCTTCACG-3' (nucleotide no. 224-243) and *Socs3* antisense primer; 5'-GTGGAGCATCATACTGATCC-3' (nucleotide no. 673-654), and *ACTB* sense primer; 5'-GGCACCACACCTTCTACAAT-3' (nucleotide no. 257-276) and *ACTB* antisense primer; 5'-AGGTCTCAAACATGATCTGG-3' (nucleotide no. 379-360). The nucleotide sequences of PCR products were confirmed using DNA sequencer as described above. Data of real-time PCR were analyzed by the $2^{-\Delta\Delta Ct}$ method (10).

In situ hybridization

Male mice (8 weeks old) were transcardially perfused with 0.9% saline followed by 4% paraformaldehyde. The brains were post-fixed overnight and then put in sucrose solution (30% in 10 mM phosphate buffer) at 4°C until they sank. The brains were cut at 16 μm thickness with a cryostat at −20°C. Digoxigenin (DIG)-labeled antisense and sense RNA probes were produced from a cloned PCR fragment (376 bp) with the sense primer: GTTCATTGTGGGAATATGCT (nucleotide no. 60-79) and the antisense primer: TCTAAGGAGCTGAGAATATGCA (nucleotide no. 435-414) using the Dig-RNA labeling kit [SP6/T7] (Roche Diagnostics). Labeling was accomplished as previously described (6, 7).

Production of NPGL and antibody against NPGL

The deduced mouse NPGL peptide containing 80 amino acid residues, identical to the rat NPGL sequence, was synthesized by microwave-assisted solid-phase peptide synthesis using an automated peptide synthesizer (Syro Wave; Biotage, Uppsala, Sweden) as previously described (11). Guinea pig and rabbit antisera were produced as previously described (6, 7)

using synthetic NPGL as the antigen. The antigen solution was mixed with Freund's complete adjuvant and injected into guinea pigs and rabbits. After a booster injection, blood was collected from each animal and the optimal serum with high titer was selected by a dot-blot analysis. Anti-NPGL antibody was purified on an NPGL-conjugated sepharose 6B column.

Immunohistochemistry

Male mice (8 weeks old) were injected with colchicine into lateral ventricle (30 μg/2.5 μl). After 2 days, the brains were cut on 20 or 60 μm sections with a cryostat at –20°C following cryoprotection and freezing. The procedure using immunoenzyme and immunofluoroscence staining on floating sections was conducted as described previously (8, 9, 12). Briefly, for the enzyme labeled antibody method, the sections were incubated in blocking buffer (1% BSA, 1% normal goat serum and 0.3% triton X-100 in 10 mM PBS) for 1 hour after incubating with 3% H_2O_2 in absolute methanol for 30 min at room temperature. Subsequently, sections were incubated in the guinea pig antibody against NPGL (1:500 dilution in blocking buffer) overnight at 4°C, and then with goat anti-guinea pig IgG (1:1000 dilution; Vector Laboratories, Burlingame, CA). Immunoreactive products were detected with an ABC kit (VECTASTAIN Elite Kit; Vector Laboratories). A control experiment was performed to examine antibody specificity by preadsorbing the working dilution of the primary antibody with a saturating concentration (10 μg/ml) of NPGL.

For the immunofluorescence method, the sections were incubated in blocking buffer (1% BSA, 1% normal donkey serum and 0.3% triton X-100 in 10 mM PBS) for 1 hour at room temperature before incubating with the rabbit antibody against NPGL (1:250 dilution in blocking buffer) overnight at 4°C. Cy3-conjugated donkey anti-rabbit IgG (1:400 dilution, 711-165-152; Jackson ImmunoResearch, West Grove, PA) was used as a secondary antibody.

Interactions of NPGL-immunoreactive fibers with NPY/AgRP or POMC neurons were surveyed using double-label immunofluorescence as follows: a guinea pig antibody against NPGL (1:500 dilution) and a rabbit antibody against AgRP (1:10,000 dilution, H-003-57; Phoenix Pharmaceuticals, Burlingame, CA) were used for the detection of NPGL fibers and NPY/AgRP neurons, and a rabbit antibody against NPGL (1:250 dilution) and a guinea pig antibody against human β-endorphin (1:2,000 dilution, T-5009; Peninsula Laboratories, San Carlos, CA) were used for the detection of NPGL fibers and POMC neurons. Cy3-conjugated donkey anti-rabbit IgG (1:400 dilution, 711-165-152; Jackson ImmunoResearch) and Alexa Fluor 488-conjugated donkey anti-guinea pig IgG (1:600 dilution, 706-545-148, Jackson ImmunoResearch) were used as secondary antibodies. Immunoreactive labeling was observed using an Eclipse E600 conventional microscope (Nikon, Tokyo, Japan) or a FV1000 confocal microscope (Olympus, Tokyo, Japan).

I.c.v. injection

Male mice (8 weeks old) were employed. A guide cannula (22 gauge, C313GS-5; Plastics One, Roanoke, VA) was fixed to the skull using acrylic resin (Shofu, Kyoto, Japan). The final coordinates of the guide cannula tips were 0.2 mm caudal to bregma, 1.0 mm lateral to midline, and 1.25 mm ventral to the skull surface. The injector (28 gauge, C313IS-5; Plastics One) was extended to 1.0 mm below the tip of the guide cannula. Injections were delivered by a syringe (Hamilton, Bonaduz, Switzerland) connected to polyethylene tubing using a syringe pump controller (BASi, West Lafayette, IN). The injection of reagents was performed after a postoperative period of 10 days. NPGL was diluted in 30% propylene glycol at pH 8.0 and the injection dose was 1.0 nmol/animal. The vehicle of 30% propylene glycol at pH 8.0 was used as a control. The injection was conducted at beginning of light period and food intake was measured at 1, 2, 4, 6, 8, 10 and 24 hours after the injection.

Measurement of serum glucose concentration

Serum glucose concentration was measured by GLUCOCARD G+ meter (Arkray, Kyoto, Japan).

Statistics

Statistically significant differences were calculated using Student's *T* test or a one-way analysis of variance (ANOVA). Differences at *P* values < 0.05 were considered statistically significant.

Results

Cloning of cDNA encoding the mouse NPGL precursor

The cDNA sequence encoding NPGL was determined using total RNA isolated from the mouse hypothalamus. The open reading frame was 546 bp, and the deduced protein consisted of 181 amino acid residues (Fig. 1A). The precursor protein includes a 33-amino acid signal peptide at the N-terminus, an 80-amino acid residue small protein, a Gly amidation signal and a dibasic cleavage site (Arg-Arg) at the C-terminus of the small protein, and an extended C-terminal sequence (Fig. 1A). In addition, NPGL contains two Cys residues, suggesting disulfide bond formation (Fig. 1A). The amino acid sequence alignment of NPGL proteins deduced from the cDNA of mouse and chicken is shown in Fig. 1B. The amino acid sequence similarity of NPGL between the mouse and chicken is 85%.

Expression of the NPGL precursor mRNA in the brain

The expression levels of the *NPGL* precursor mRNA within different regions of the brain, including the telencephalon, diencephalon, mesencephalon, cerebellum, and MBH were

examined by real-time RT-PCR. The *NPGL* precursor mRNA was exclusively expressed in the MBH, whereas expression in other brain regions was around background levels (Fig. 2).

Morphological analysis

The localization of the NPGL-containing cells in the brain was further analyzed by *in situ* hybridization and immunohistochemistry. Figure 3A schematically shows the localization of NPGL-containing cell bodies (closed dots) and fibers (open dots) in the MBH. *In situ* hybridization revealed that cells expressing the *NPGL* precursor mRNA were specifically distributed in the lateroposterior part of the Arc (ArcLP) within the MBH (Fig. 3, B and C). Positive signals were detected by the antisense probe (Fig. 3, B and C), but not by the sense probe (Fig. 3D). Immunohistochemistry also showed that NPGL-immunoreactive cell bodies and fibers were localized in the ArcLP within the MBH (Fig. 3E). Cell and fiber labeling were absent in preadsorption experiments (Fig. 3F). The colchicine treatment enabled the detection of NPGL-immunereactive cells. NPGL-immunoreactive fibers were distributed in the lateral part of the Arc (ArcL), around the ventromedial hypothalamus (VMH), near the third ventricle (Fig. 3, G and H), and between the dorsomedial hypothalamus (DMH) and the posterior hypothalamus (PH) (Fig. 3, A, G and H).

The interactions of NPGL neurons with other well-known neuropeptides regulating feeding, i.e., NPY/AgRP or POMC neurons, were investigated in the rostral regions of the Arc. NPGL-immunoreactive fibers were found in close apposition to POMC neurons in the ArcL but not NPY/AgRP neurons (Fig. 4). Using confocal microscopy, NPGL-immunoreactive fibers were found to contact POMC neurons (Fig. 4, F–H).

Expression of the NPGL precursor mRNA under fasting

As the location of NPGL cell bodies and projections in the hypothalamus pointed to a potential role for this protein in energy metabolic regulation (13), we examined the response of NPGL to a negative energy balance. The expression of *NPGL* precursor mRNA was examined after 24 h of fasting. The expression level of *NPGL* was significantly higher in fasted mice relative to non-fasted mice (Fig. 5A). Although both fasted and non-fasted mice showed similar serum glucose levels (Fig. 5B), body weight significantly decreased in fasted mice (Fig. 5C).

Expression of the NPGL precursor mRNA under short- or long-term exposure to HFD

The increased expression of *NPGL* in fasted mice, suggested that this protein may serve to signal a negative energy balance. To further examine this possibility, we explored whether *NPGL* expression would be decreased during a positive energy state. When mice were fed HFD for 5 weeks beginning at 4 weeks of age, the expression level of the *NPGL* precursor mRNA was significantly reduced in HFD-fed mice (Fig. 6A). It is known that HFD intake

induces an increase in a hypothalamic suppressor of cytokine signaling 3 (Socs3) that serves to inhibit leptin signaling, eventually leading to obesity in HFD-fed mice (14). Therefore, we measured the *Socs3* mRNA expression level and body weight in normal chow (NC)- and HFD-fed mice. Contrary to expectation, significant differences were not detected in both parameters (Fig. 6, B and C). However, serum glucose levels were significantly elevated in HFD-fed mice (Fig. 6D).

When mice were fed HFD for 13 weeks beginning at 4 weeks of age, *NPGL* precursor mRNA expression levels in HFD-fed mice did not differ from that of control mice (Fig. 6E). *Socs3* mRNA expression levels and body weight significantly increased in HFD-fed mice (Fig. 6, F and G). Serum glucose levels were significantly higher in HFD-fed mice than in NC-fed mice, as well as mice fed for 5 weeks (Fig. 6H)

Effect of NPGL on food intake

Because *NPGL* precursor mRNA expression levels were up-regulated by fasting and down-regulated by short-term HFD feeding, we predicted that *NPGL* acts as an orexigenic neuropeptides in mice. To examine this possibility, we administrated NPGL, mature protein, into the lateral ventricle at the beginning of light period, and measured food intake at 1, 2, 4, 6, 8, 10 and 24 hours after the i.c.v. injection. Cumulative food intake significantly increased about 2.5 times after 2 hours from the injection, and about 2 times after 4, 6, 8 and 10 hours (Fig. 7A). A significant difference was not detected after 24 hours from the injection (Fig. 7A). Food intake per unit time significantly increased 3.3 times from 1 to 2 hour, 2.9 times from 4 to 6 hour and 1.6 times from 6 to 8 hour after injection (Fig. 7B). This result indicates that the orexigenic effect of NPGL deteriorated over time but was sustained for at least 8 hours (Fig. 7B).

Discussion

We have recently reported that the mRNA encoding NPGL, a novel hypothalamic small secretory protein, is expressed in the chicken hypothalamus, and NPGL may participate in the growth process in chicks (5). We speculated that the NPGL precursor gene is conserved in vertebrates, including mammals, a possibility confirmed via a database search (5). The present study shows, for the first time, the cloning of *NPGL* cDNA and the identification of NPGL neurons in the mammalian brain. Furthermore, *NPGL* precursor mRNA expression levels are elevated by fasting and reduced by short-term HFD feeding, and central injections of NPGL increase food intake. Together, these results suggest that NPGL is a novel orexigenic neuropeptide in mice.

Quantitative RT-PCR and morphological analyses revealed that NPGL neurons are located in the ArcLP within the MBH. The rostral region of the Arc in the hypothalamus is

one of the centers of energy metabolic regulation and contains two major neuronal populations (i.e., NPY/AgRP neurons and POMC neurons; 2, 15). NPY/AgRP neurons promote food intake and decrease energy expenditure, whereas POMC neurons have the opposite effect (13). mRNA expression levels of NPY and POMC change in response to energetic status in order to maintain energy homeostasis (13). In the present study, double-label immunofluorescence revealed that NPGL-immunoreactive fibers form close contacts with POMC neurons in the ArcL. This result suggests that NPGL may stimulate feeding behavior through inhibition of anorexigenic POMC neurons. In addition to the ArcL, NPGL neuronal fibers were also observed in the DMH and VMH. Several neuropeptidergic cell phenotypes that regulate food intake are distributed in the DMH and VMH. In particular, a population of NPY cells is found in the DMH in addition to the ArcL (16). NPY cells in this region, as well as in the ArcL, stimulate food intake (17). A few cell bodies expressing melanin-containing hormone (MCH) and orexin/hypocretin are also found in the DMH, although the majority of these cells are located in the lateral hypothalamic area (LHA) (18). Both MCH and orexin/hypocretin neurons promote food intake (19, 20). In the VMH, pituitary adenylate cyclase-activating polypeptide (PACAP) cells are expressed 21) and central injections of PACAP inhibit food intake (22). Thus, NPGL may regulate food intake by acting via these well-established mechanisms of energetic control.

A negative energy balance induced by fasting elevated the expression of *NPGL* precursor mRNA, suggesting that NPGL has orexigenic properties in mice. As mentioned previously, fasting increases orexigenic neuropeptides such as NPY (23, 24) and agouti-related protein (AgRP) (24, 25). Further support for an orexigenic role of NPGL comes from the fact that injection of NPGL increased food intake. Because serum glucose levels were not affected by fasting in this study, it is likely that changes in *NPGL* expression are not a result of changes in glucose. In contrast, HFD feeding for 5 weeks, but not 13 weeks (a positive energy balance) reduced the expression of *NPGL* precursor mRNA. Extended maintenance on a HFD impairs central leptin sensitivity, increases body weight, and inevitably leads to leptin resistance and obesity (26, 27), in part, through increased hypothalamic *Socs3* expression (14, 28). In the present study, short-term (5 weeks) HFD significantly decreased *NPGL* precursor mRNA without affecting body weight and *Socs3* mRNA expression. This result suggests that leptin continues to play an anti-obesity role in short-term HFD fed-mice to prevent diet-induced obesity (DIO). These findings suggest that NPGL neurons are responsive to leptin at this point. By contrast, in long-term (13 weeks) HFD fed-mice, *NPGL* precursor mRNA expression was not different from control levels, although *Socs3* mRNA and body weight were increased. This result suggests that leptin resistance occurs in this stage. Taken together, these results point to the possibility that *NPGL* mRNA expression is reduced by leptin in

short-term HFD fed-mice, and this reduction is not observed in long-term HFD fed-mice due to leptin resistance. In both short- and long-term HFD-fed mice, serum glucose levels were increased. This result suggests that serum glucose levels do not influence the expression of *NPGL*. Whether or not NPGL cells are directly responsive to leptin represents an important avenue for further enquiry.

In summary, the present findings report on the cDNA encoding NPGL in the mouse hypothalamus, representing the first characterization of this neurochemical in the mammalian brain. NPGL neurons are localized to the ArcLP with fibers projecting to several areas of the hypothalamus mediating food intake and energy homeostasis, and especially POMC neurons. The mRNA expression level of the *NPGL* precursor is markedly, and predictably, impacted by energetic status and central injections of NPGL increase food intake. Together, these findings point to NPGL as a novel orexigenic neuropeptide in mice and an important target for further study to fully understand the central mechanisms regulating energy homeostasis.

Acknowledgements

We are grateful to Dr. Akiko K. Satoh (Hiroshima University) for her invaluable assistance with confocal microscopy. This work was supported by grants from MEXT/JSPS KAKENHI (22687004, 23126517, 25126717, 26291066, and 15KK0259 to K.U., and 25440171 and 16K07440 to E.I.-U.), Grant-in-Aid for JSPS Fellows (15J03781 to K.S.), the Program for Promotion of Basic and Applied Research for Innovations in Bio-oriented Industry (K.U.), the Toray Science Foundation (K.U.), the Mishima Kaiun Memorial Foundation (K.U. and E.I.-U.), the Suzuken Memorial Foundation (K.U.), the SKYLARK Food Science Institute (K.U.), the Urakami Foundation for Food and Food Culture Promotion (K.U.), and the Kao Research Council for the Study of Healthcare Science (K.U.).

[#]*Corresponding author and person to whom reprint requests should be addressed*: Kazuyoshi Ukena, Ph.D., Professor, Section of Behavioral Sciences, Graduate School of Integrated Arts and Sciences, Hiroshima University, Higashi-Hiroshima 739-8521, Japan, Phone: +81-82-424-6571, Fax: +81-82-424-0759, e-mail: ukena@hiroshima-u.ac.jp

The sequence reported in this paper has been deposited in the GenBank database (accession no. LC088498) for the cDNA sequence of mouse NPGL precursor polypeptide.

Disclosure Summary: The authors of this manuscript have nothing to disclose.

Disclosure Statement: The authors have nothing to disclose.

References

1. **Zhang Y, Proenca R, Maffei M, Barone M, Leopold L, Friedman JM.** Positional cloning of the mouse obese gene and its human homologue. *Nature*. 1994; 372:425–432.
2. **Elias CF, Aschkenasi C, Lee C, Kelly J, Ahima RS, Bjorbaek C, Flier JS, Saper CB, Elmquist JK.** Leptin differentially regulates NPY and POMC neurons projecting to the lateral hypothalamic area. *Neuron*. 1999; 23:775–786.
3. **Shintani M, Ogawa Y, Ebihara K, Aizawa-Abe M, Miyanaga F, Takaya K, Hayashi T, Inoue G, Hosoda K, Kojima M, Kangawa K, Nakao K.** Ghrelin, an endogenous growth hormone secretagogue, is a novel orexigenic peptide that antagonizes leptin action through the activation of hypothalamic neuropeptide Y/Y1 receptor pathway. *Diabetes*. 2001; 50:227–232.
4. **Sakurai T.** The neural circuit of orexin (hypocretin): maintaining sleep and wakefulness. *Nat Rev Neurosci*. 2007; 8:171–181.
5. **Ukena K, Iwakoshi-Ukena E, Taniuchi S, Bessho Y, Maejima S, Masuda K, Shikano K, Kondo K, Furumitsu M, Tachibana T.** Identification of a cDNA encoding a novel small secretory protein, neurosecretory protein GL, in the chicken hypothalamic infundibulum. *Biochem Biophys Res Commun*. 2014; 446:298–303.
6. **Ukena K, Iwakoshi-Ukena E, Hikosaka A.** Unique form and osmoregulatory function of a neurohypophysial hormone in a urochordate. *Endocrinology*. 2008; 149:5254–5261.
7. **Ukena K, Tachibana T, Iwakoshi-Ukena E, Saito Y, Minakata H, Kawaguchi R, Osugi T, Tobari Y, Leprince J, Vaudry H, Tsutsui K.** Identification, localization, and function of a novel avian hypothalamic neuropeptide, 26RFa, and its cognate receptor, G protein-coupled receptor-103. *Endocrinology*. 2010; 151:2255–2264.
8. **Kriegsfeld LJ, Mei DF, Bentley GE, Ubuka T, Mason AO, Inoue K, Ukena K, Tsutsui K, Silver R.** Identification and characterization of a gonadotropin-inhibitory system in the brains of mammals. *Proc Natl Acad Sci USA*. 2006; 103:2410–2415.
9. **Ubuka T, Inoue K, Fukuda Y, Mizuno T, Ukena K, Kriegsfeld LJ, Tsutsui K.** Identification, expression, and physiological functions of Siberian hamster gonadotropin-inhibitory hormone. *Endocrinology*. 2012; 153:373–385.
10. **Livak KJ, Schmittgen TD.** Analysis of relative gene expression data using real-time quantitative PCR and the $2^{-\Delta\Delta Ct}$ Method. *Methods*. 2001; 25:402–408.
11. **Masuda K, Ooyama H, Shikano K, Kondo K, Furumitsu M, Iwakoshi-Ukena E, Ukena K.** Microwave-assisted solid-phase peptide synthesis of neurosecretory protein GL composed of 80 amino acid residues. *J Pept Sci*. 2015; 21:454–460.

12. **Ukena K, Usui M, Kohchi C, Tsutsui K.** Cytochrome P450 side-chain cleavage enzyme in the cerebellar Purkinje neuron and its neonatal change in rats. *Endocrinology*. 1998; 139:137–147.
13. **Barsh GS, Schwartz MW.** Genetic approaches to studying energy balance: perception and integration. *Nat Rev Genet*. 2002; 3:589–600.
14. **Gamber KM, Huo L, Ha S, Hairston JE, Greeley S, Bjørbæk C.** Over-expression of leptin receptors in hypothalamic POMC neurons increases susceptibility to diet-induced obesity. *PLOS One*. 2012; 7:e30485.
15. **Waterson MJ, Horvath TL.** Neuronal regulation of energy homeostasis: beyond the hypothalamus and feeding. *Cell Metab*. 2015; 22:962–970.
16. **Bi S, Robinson BM, Moran TH.** Acute food deprivation and chronic food restriction differentially affect hypothalamic NPY mRNA expression. *Am J Physiol Regul Integr Comp Physiol*. 2003; 285:R1030–1036.
17. **Yang L, Scott KA, Hyun J, Tamashiro KL, Tray N, Moran TH, Bi S.** Role of dorsomedial hypothalamic neuropeptide Y in modulating food intake and energy balance. *J Neurosci*. 2009; 29:179–190.
18. **Leinninger GM.** Lateral thinking about leptin: a review of leptin action via the lateral hypothalamus. *Physiol Behav*. 2011; 104:572–581.
19. **Qu D, Ludwig DS, Gammeltoft S, Piper M, Pelleymounter MA, Cullen MJ, Mathes WF, Przypek R, Kanarek R, Maratos-Flier E.** A role for melanin-concentrating hormone in the central regulation of feeding behaviour. *Nature*. 1996; 380:243–247.
20. **Sakurai T, Amemiya A, Ishii M, Matsuzaki I, Chemelli RM, Tanaka H, Williams SC, Richardson JA, Kozlowski GP, Wilson S, Arch JR, Buckingham RE, Haynes AC, Carr SA, Annan RS, McNulty DE, Liu WS, Terrett JA, Elshourbagy NA, Bergsma DJ, Yanagisawa M.** Orexins and orexin receptors: a family of hypothalamic neuropeptides and G protein-coupled receptors that regulate feeding behavior. *Cell*. 1998; 92:573–585.
21. **Hawke Z, Ivanov TR, Bechtold DA, Dhillon H, Lowell BB, Luckman SM.** PACAP neurons in the hypothalamic ventromedial nucleus are targets of central leptin signaling. *J Neurosci*. 2009; 29:14828–14835.
22. **Mounien L, Do Rego JC, Bizet P, Boutelet I, Gourcerol G, Fournier A, Brabet P, Costentin J, Vaudry H, Jégou S.** Pituitary adenylate cyclase-activating polypeptide inhibits food intake in mice through activation of the hypothalamic melanocortin system. *Neuropsychopharmacology*. 2009; 34:424–435.

23. **Bergen HT, Mobbs CV.** Ventromedial hypothalamic lesions produced by gold thioglucose do not impair induction of NPY mRNA in the arcuate nucleus by fasting. *Brain Res*. 1996; 707:266–271.
24. **Mizuno TM, Makimura H, Silverstein J, Roberts JL, Lopingco T, Mobbs CV.** Fasting regulates hypothalamic neuropeptide Y, agouti-related peptide, and proopiomelanocortin in diabetic mice independent of changes in leptin or insulin. *Endocrinology*. 1999; 140:4551–4557.
25. **Hahn TM, Breininger JF, Baskin DG, Schwartz MW.** Coexpression of Agrp and NPY in fasting-activated hypothalamic neurons. *Nat Neurosci*. 1998; 1:271–272.
26. **Mu¨nzberg H, Flier JS, Bjørbaek C.** Region-specific leptin resistance within the hypothalamus of diet-induced obese mice. *Endocrinology*. 2004; 145:4880–4889.
27. **El-Haschimi K, Pierroz DD, Hileman SM, Bjørbaek C, Flier JS.** Two defects contribute to hypothalamic leptin resistance in mice with diet-induced obesity. *J Clin Invest*. 2000; 105:1827–1832.
28. **Thaler JP, Schwartz MW.** Minireview: Inflammation and obesity pathogenesis: the hypothalamus heats up. *Endocrinology*. 2010; 151:4109–4115.

FIG. 1. Nucleotide sequence and amino acid sequence of the NPGL precursor in mouse (A). The predicted signal peptide is denoted by a wavy line. The Gly (G) C-terminal amidation signal and the Arg (R)-Arg (R) dibasic processing site are underlined. The predicted 80-amino acid residue mature protein is present in boldface. Two Cys (C) residues are boxed. The stop codon (TAA) is indicated by the asterisk. Amino acid sequence alignment of NPGL precursor deduced from mouse and chicken cDNA sequences (B). A hyphen was inserted in one gap to optimize the sequence alignment. Gray boxes highlight conserved amino acids. The predicted mature small proteins are underlined. The conserved two Cys (C) residues are indicated by asterisks.

FIG. 2. Real-time RT-PCR analysis of *NPGL* precursor mRNA concentrations in different brain regions. *NPGL* precursor mRNA levels were quantified relative to the level of β-actin (ACTB) mRNA. Each value represents the mean ± SEM (n = 4). Asterisks indicate a statistically significant difference (**$P < 0.001$).

FIG. 3 (Color online). NPGL-containing cell bodies and fibers in the hypothalamus are represented by closed and open dots in the schematic illustrations, respectively (A). Photomicrographs of cells expressing *NPGL* precursor mRNA were obtained by *in situ* hybridization in the lateroposterior part of the arcuate hypothalamic nucleus (ArcLP) within the mediobasal hypothalamus (B and C, C is enlarged view of B). No signals were detected

using the sense probe (D). Photomicrographs of NPGL-immunoreactive cells and fibers were obtained by immunohistochemistry in the same region as *in situ* hybridization (E-H). No signals were detected when the primary antibody was preadsorbed with the antigenic peptide (F). NPGL-immunoreactive fibers were also detected in the lateral part of the arcuate nucleus (ArcL), around the ventromedial hypothalamus (VMH), near the third ventricle (3v), and between the dorsal part of the dorsomedial hypothalamus (DMH) and the posterior hypothalamus (PH) (A, G, and H). Scale bars = 100 µm.

FIG. 4. The regions shown in the photomicrographs (B and D) depicted in the schematic illustration (A). Distribution of NPGL-immunoreactive fibers in the vicinity of NPY/AgRP neurons (B and C) and POMC neurons (D–H) in the rostral region of the arcuate nucleus using conventional microscopy (B–E) or confocal microscopy (F–H). The dotted squares in B and D are shown magnified in C, E, and F. Arrowheads in B and D indicate NPY/AgRP neurons (B) and POMC neurons (D). Arrows in E–H show NPGL-immunoreactive fibers in contact with POMC neurons (E–H). Triangles in G indicate descending NPGL-immunoreactive fibers (G). Scale bars = 100 µm in B and D, and 10 µm in C and E–H.

FIG. 5. Effects of 24 h of food deprivation (FD) on the expression of *NPGL* precursor mRNA (A), serum glucose concentration (B) and body weight (C). CTL = control experiment. Each value represents the mean ± SEM (n = 6). Asterisks indicate statistically significant differences (*$P < 0.05$, **$P < 0.001$).

FIG. 6. Effects of normal chow (NC) or high fat diet (HFD) feeding for 5 (A-D) or 13 weeks (E-H) beginning at 4 weeks of age on the expression of *NPGL* precursor mRNA (A, E), *Socs3* mRNA (B, F), body weight (C, G) and serum glucose concentration (D, H). Each value represents the mean ± SEM (n = 5-6). Asterisks indicate statistically significant differences (*$P < 0.05$, **$P < 0.001$).

FIG. 7. Effect of intracerebroventricular injection of vehicle or NPGL (1.0 nmol/animal) on food intake. Data are shown as cumulative food intake after the injection (A) and per unit time (B). Each value represents the mean ± SEM (n = 8-10). Asterisks indicate statistically significant differences (*$P < 0.05$).

Peptide/protein target	Antigen sequence (if known)	Name of Antibody	Manufacturer, catalog #, and/or name of individual providing the antibody	Species raised in; monoclonal or polyclonal	Dilution used	RRID (required in revised MSs)
NPGL	HSQTDLLTLNQADPQCWESSSMLL LEMRKPRVSNTVSGFWDFMIYLKS SENLKHGALFWDLAQLFWDIYVDC VLSRNHGL-NH2	Anti-NPGL	Our lab	Guinea pig; polyclonal	1/500	AB_2636992
NPGL	HSQTDLLTLNQADPQCWESSSMLL LEMRKPRVSNTVSGFWDFMIYLKS SENLKHGALFWDLAQLFWDIYVDC VLSRNHGL-NH2	Anti-NPGL	Our lab	Rabbit; polyclonal	1/250	AB_2636993
Human beta-endorphin		Anti-beta-Endorphin	Peninsula Laboratories, T-5009	Guinea pig; polyclonal	1/2000	AB_518107
Agouti-related protein		Anti-AgRP	Phoenix Pharmaceuticals, H-003-57	Rabbit; polyclonal	1/10000	AB_2313909
Guinea pig IgG		Biotinylated goat anti-guinea pig IgG	Vector Labs, BA-7000	Goat; polyclonal	1/1000	AB_2336132
Rabbit IgG		Cy3-conjugated donkey anti-rabbit IgG	Jackson Immunoresearch, 711-165-152	Donky; polyclonal	1/400	AB_2307443
Guinea pig IgG		Alexa Fluor 488-conjugated donkey anti-guinea pig IgG	Jackson Immunoresearch, 706-545-148	Donky; polyclonal	1/600	AB_2340472

A

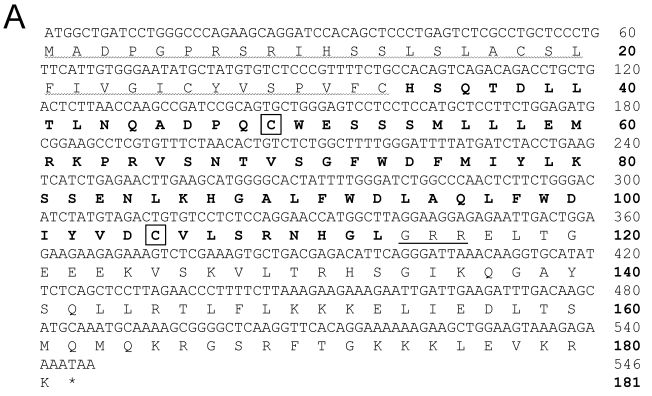

B

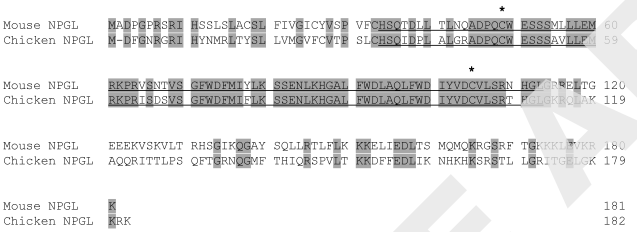

Fig.1

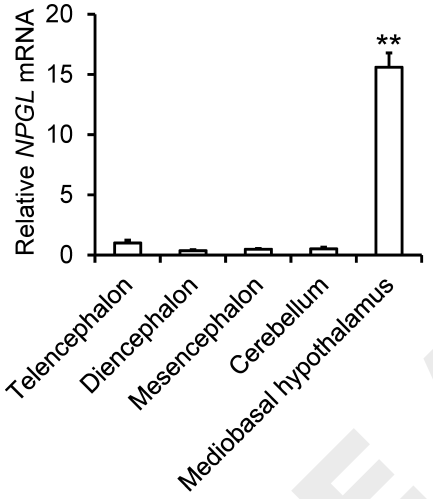

Fig.2

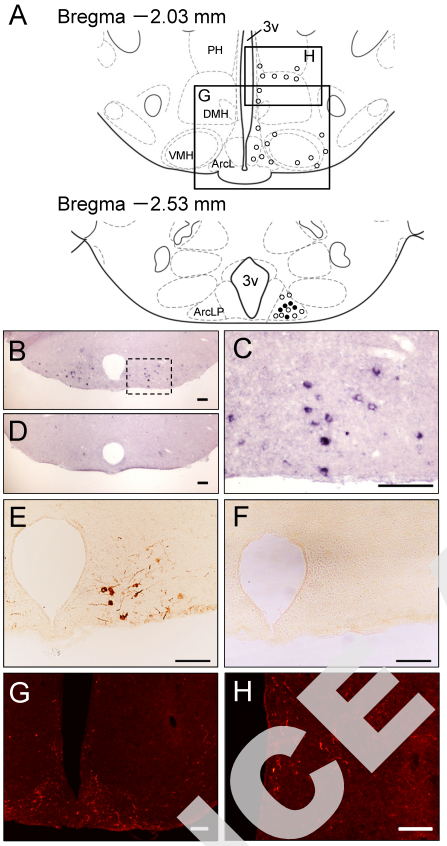

Fig.3

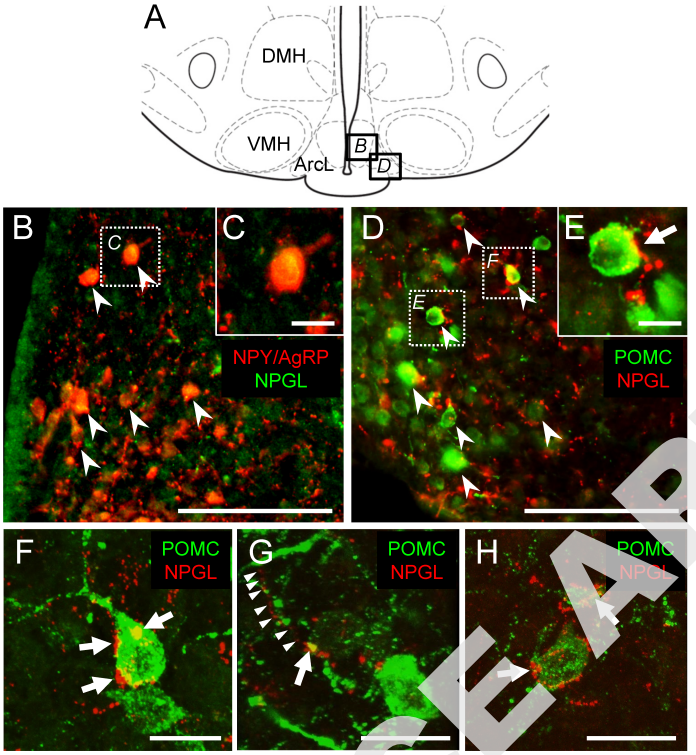

Fig.4

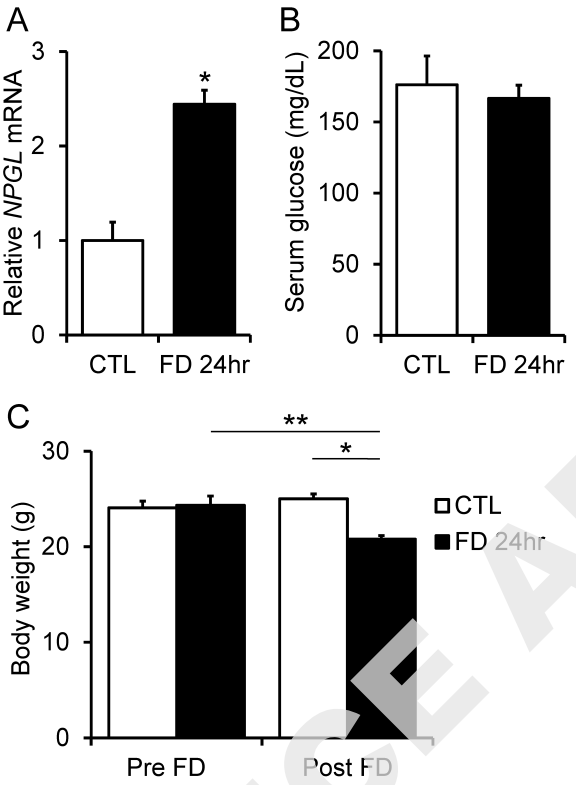

Fig.5

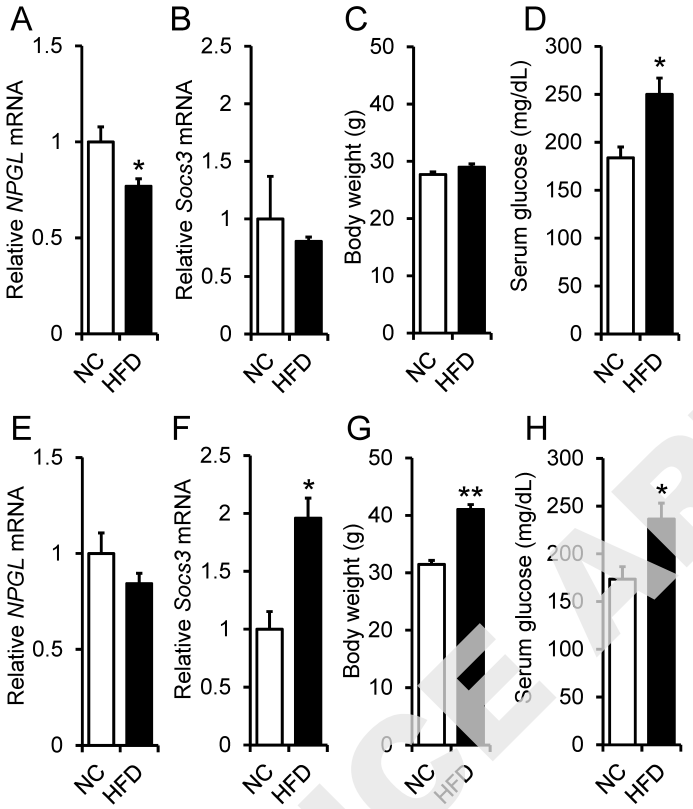

Fig.6

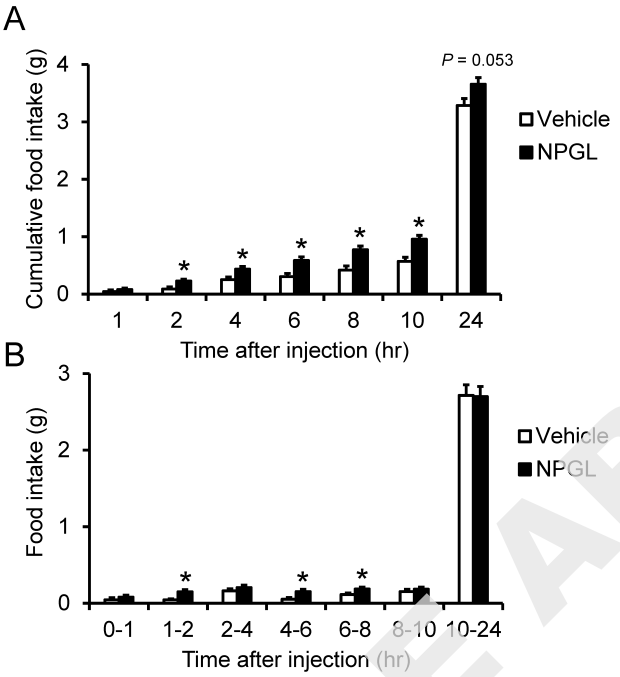

Fig.7